Insights into pyridine-based graphynes anchoring with second-row transition metal single atoms for electrocatalytic CO_2 reduction: a DFT study

Decheng Peng[ab], Xin Li[*ac], Liangfu Zhao[a], Jiangang Chen[a], and Qiang Wang[*a]

[a] State Key Laboratory of Coal Conversion, Institute of Coal Chemistry, Chinese Academy of Sciences, Taiyuan 030001, China
[b] Taiyuan University of Technology, Taiyuan 030024, China
[c] University of Chinese Academy of Sciences, Beijing 100049, China

E-mail address: wqiang@sxicc.ac.cn

Corresponding author: Qiang Wang, Xin Li.

Table S1. The TM-N bond length of first row and second row transition metal, TM-N difference and covalent radius difference.

Catalyst	TM-N-4d (Å)	TM-N-3d (Å)	TM-N difference (Å)	Covalent radius difference, (Å)
Y/Sc-pdGY	2.21	2.16	0.05	0.15
Zr/Ti-pdGY	2.17	2.13	0.04	0.18
Nb/V-pdGY	2.12	2.05	0.07	0.13
Mo/Cr-pdGY	2.10	2.04	0.06	0.16
Tc/Mn-pdGY	2.08	2.00	0.08	0.09
Ru/Fe-pdGY	2.05	2.00	0.05	0.09
Rh/Co-pdGY	2.04	1.97	0.07	0.14
Pd/Ni-pdGY	2.05	1.95	0.1	0.1
Ag/Cu-pdGY	2.09	1.97	0.12	0.16
Cd/Au-pdGY	2.09	1.97	0.12	0.18

Table S2. The formation energy (E_f), binding energy(E_b), cohesive energy (E_{coh}), and Bader charge of TM atoms on TM-pdGYs.

Catalyst	E_f (eV)	E_b (eV)	E_{coh} (eV)	Charge (|e|)
Y-pdGY	-1.63	-5.80	-4.18	2.02
Zr-pdGY	0.33	-5.92	-6.26	1.50
Nb-pdGY	2.1	-4.71	-6.89	1.24
Mo-pdGY	2.50	-3.72	-6.22	0.88
Tc-pdGY	2.63	-4.29	-6.92	0.94
Ru-pdGY	2.65	-4.94	-7.59	0.65
Rh-pdGY	1.48	-4.36	-5.83	0.48
Pd-pdGY	0.46	-3.29	-3.75	0.35
Ag-pdGY	-0.39	-2.89	-2.50	0.53
Cd-pdGY	-0.12	-0.82	-0.70	1.08

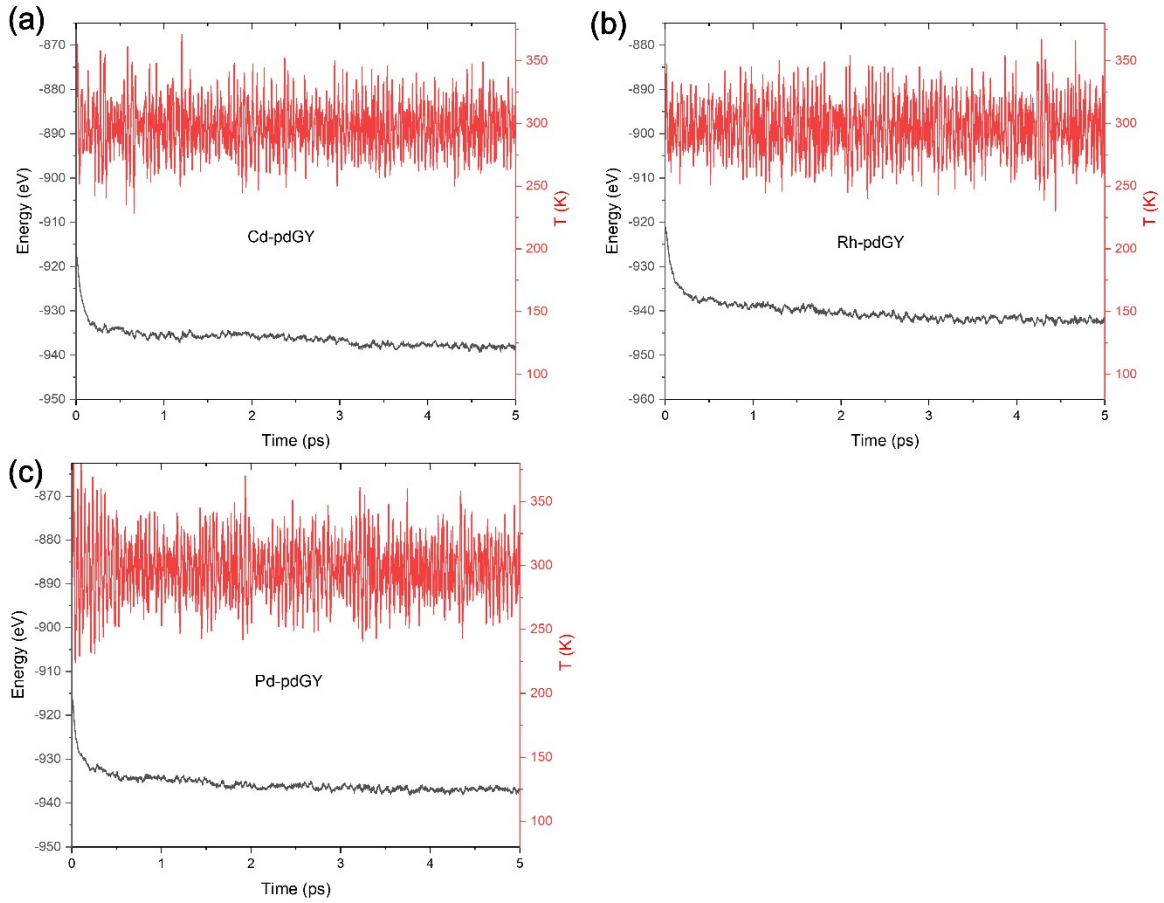

Fig.S1. The changes in energy and temperature within 5 ps of (a) Cd-pdGY, (b) Rh-pdGY and (c) Pd-pdGY by AIMD simulation.

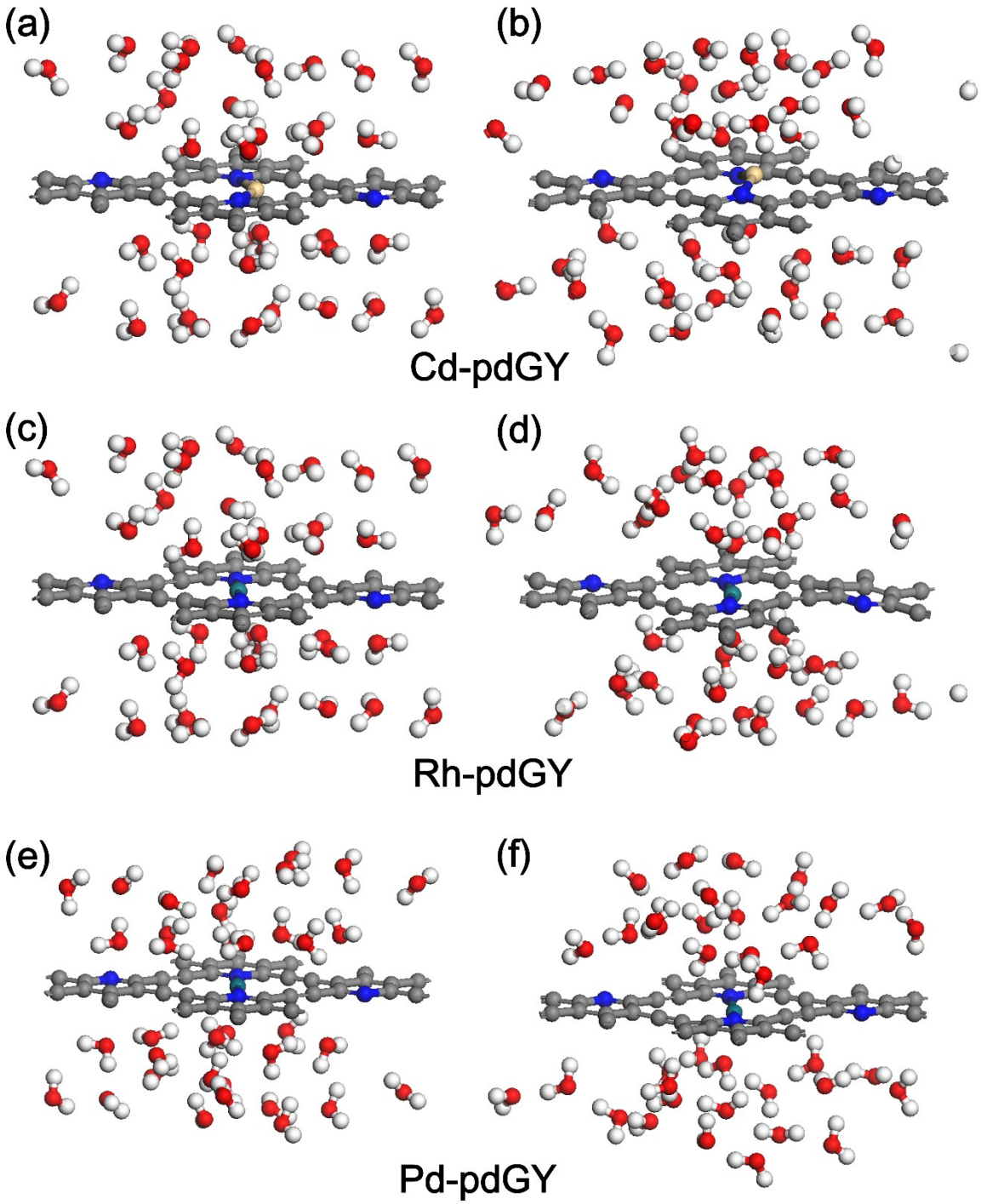

Fig.S2. The configurations of Cd/Rh/Pd-pdGY before (a, c and e) and after (b, d and f) AIMD simulations.

Table S3. The adsorption energies of CO_2 and H atoms on TM-pdGYs

Catalyst	$E_{ad}(CO_2)$ (eV)	$E_{ad}(H)$ (eV)
Y-pdGY	-0.94	-0.61
Zr-pdGY	-1.75	-0.71
Nb-pdGY	-1.85	-0.55
Mo-pdGY	-3.00	-0.33
Tc-pdGY	-0.56	-0.41
Ru-pdGY	-0.68	-0.66
Rh-pdGY	-0.37	-0.60
Pd-pdGY	-0.20	-0.12
Ag-pdGY	-0.15	1.45
Cd-pdGY	-0.28	-0.95

Table S4. The adsorption free energies of CO_2 and H_2O on TM-pdGYs in implicit solvent models

Catalyst	$G_{ad}(CO_2)$ (eV)	$G_{ad}(H_2O)$ (eV)
Y-pdGY	2.14	0.61
Zr-pdGY	0.13	-0.07
Nb-pdGY	-0.32	0.23
Mo-pdGY	-0.71	-0.29
Tc-pdGY	-0.36	0.39
Ru-pdGY	-0.47	-1.35
Rh-pdGY	-0.08	-0.95
Pd-pdGY	0.21	-0.90
Ag-pdGY	0.24	-0.89
Cd-pdGY	0.28	-1.04

Table S5 The potential limited step and corresponding ΔG_{max} to generate CO on TM-pdGYs.

Catalyst	PLS	ΔG_{max}, (eV)
Y-pdGY	*CO→*+CO	0.80
Zr-pdGY	*CO→*+CO	1.45
Nb-pdGY	*CO→*+CO	2.09
Mo-pdGY	*CO→*+CO	1.28
Tc-pdGY	*CO→*+CO	1.95
Ru-pdGY	*CO→*+CO	2.22
Rh-pdGY	*CO→*+CO	1.75
Pd-pdGY	*CO→*+CO	0.75
Ag-pdGY	*CO_2+H→*COOH	1.35
Cd-pdGY	*CO_2+H→*COOH	0.12

Table S6. The adsorption energies of CO and COOH on TM-pdGYs.

Catalyst	E_{ad}(CO) (eV)	E_{ad}(COOH) (eV)
Y-pdGY	-1.1	-4.01
Zr-pdGY	-1.8	-4.16
Nb-pdGY	-2.49	-4.18
Mo-pdGY	-1.66	-3.00
Tc-pdGY	-2.33	-3.26
Ru-pdGY	-2.62	-3.50
Rh-pdGY	-2.14	-3.40
Pd-pdGY	-1.08	-2.80
Ag-pdGY	-0.19	-1.31
Cd-pdGY	-0.30	-2.61

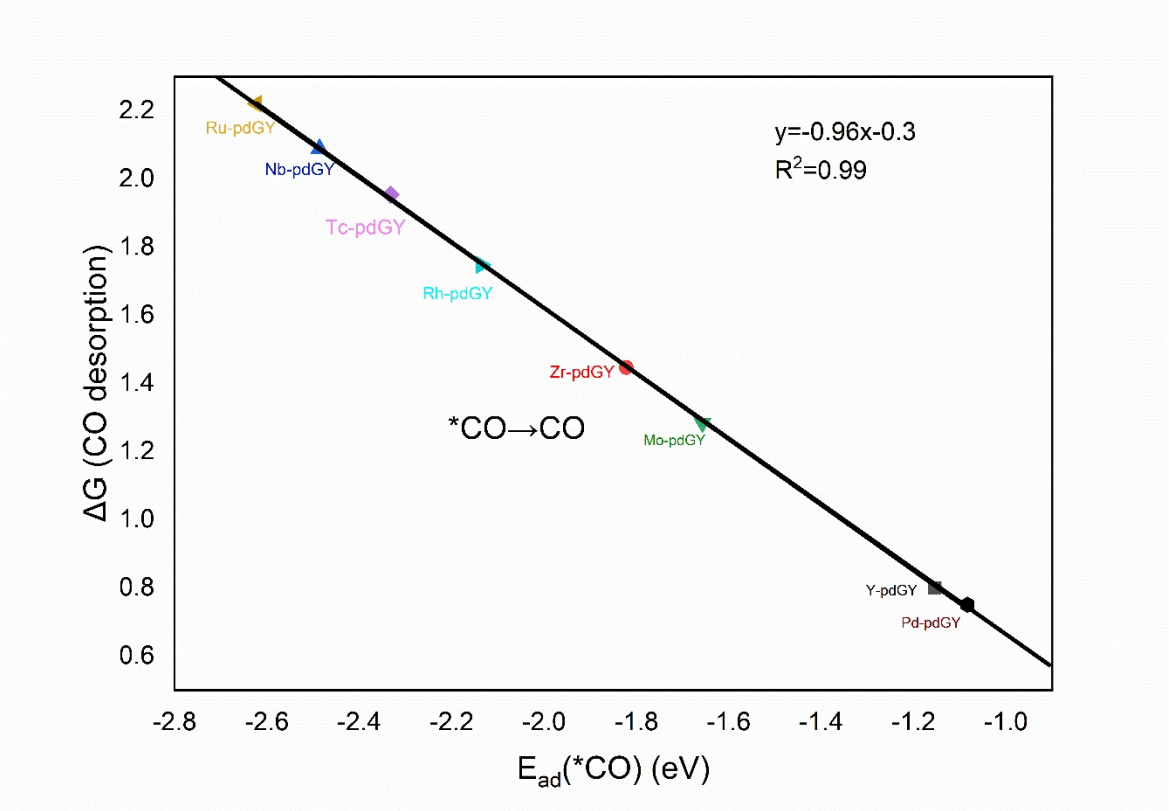

Fig.S3. The linear graph between ΔG (CO desorption) and E_{ad}[*CO]

Table S7 The potential limited step and corresponding ΔG_{max} to generate HCOOH on TM-pdGYs.

Catalyst	PLS	ΔG_{max}, (eV)
Y-pdGY	$*OCHO+H^{+}+e^{-}\rightarrow *HCOOH$	1.62
Zr-pdGY	$*OCHO+H^{+}+e^{-}\rightarrow *HCOOH$	1.50
Nb-pdGY	$*OCHO+H^{+}+e^{-}\rightarrow *HCOOH$	1.56
Mo-pdGY	$*OCHO+H^{+}+e^{-}\rightarrow *HCOOH$	0.89
Tc-pdGY	$*COOH+H^{+}+e^{-}\rightarrow *HCOOH$	0.70
Ru-pdGY	$*COOH+H^{+}+e^{-}\rightarrow *HCOOH$	0.68
Rh-pdGY	$*COOH+H^{+}+e^{-}\rightarrow *HCOOH$	0.81
Pd-pdGY	$*COOH+H^{+}+e^{-}\rightarrow *HCOOH$	0.42
Ag-pdGY	$*CO_2+H^{+}+e^{-}\rightarrow *OCHO$	1.07
Cd-pdGY	$*HCOOH\rightarrow *+HCOOH$	0.51

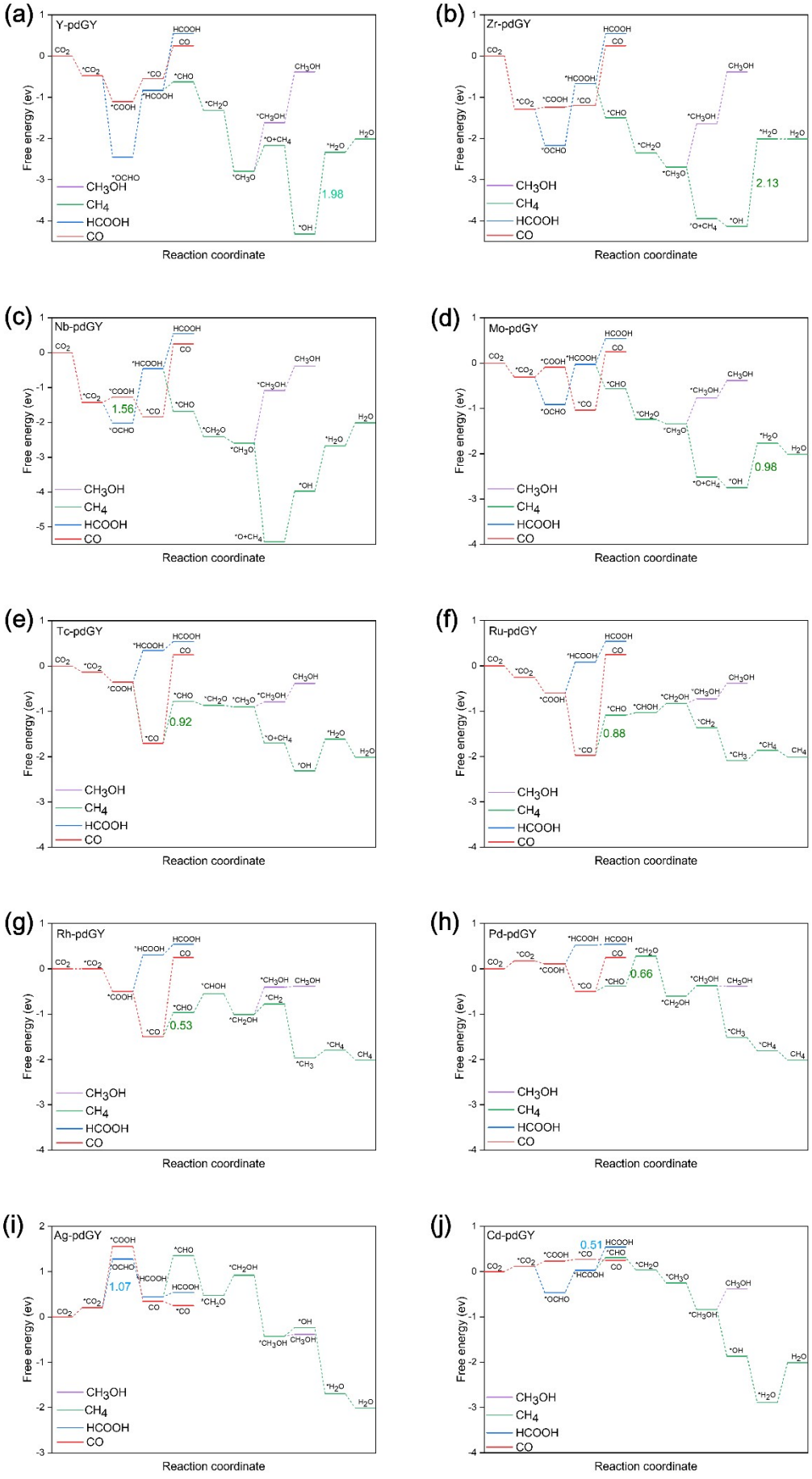

Fig.S4. The overall Gibbs free energy pathway graphs including four main products (CO, HCOOH, CH_3OH and CH_4).

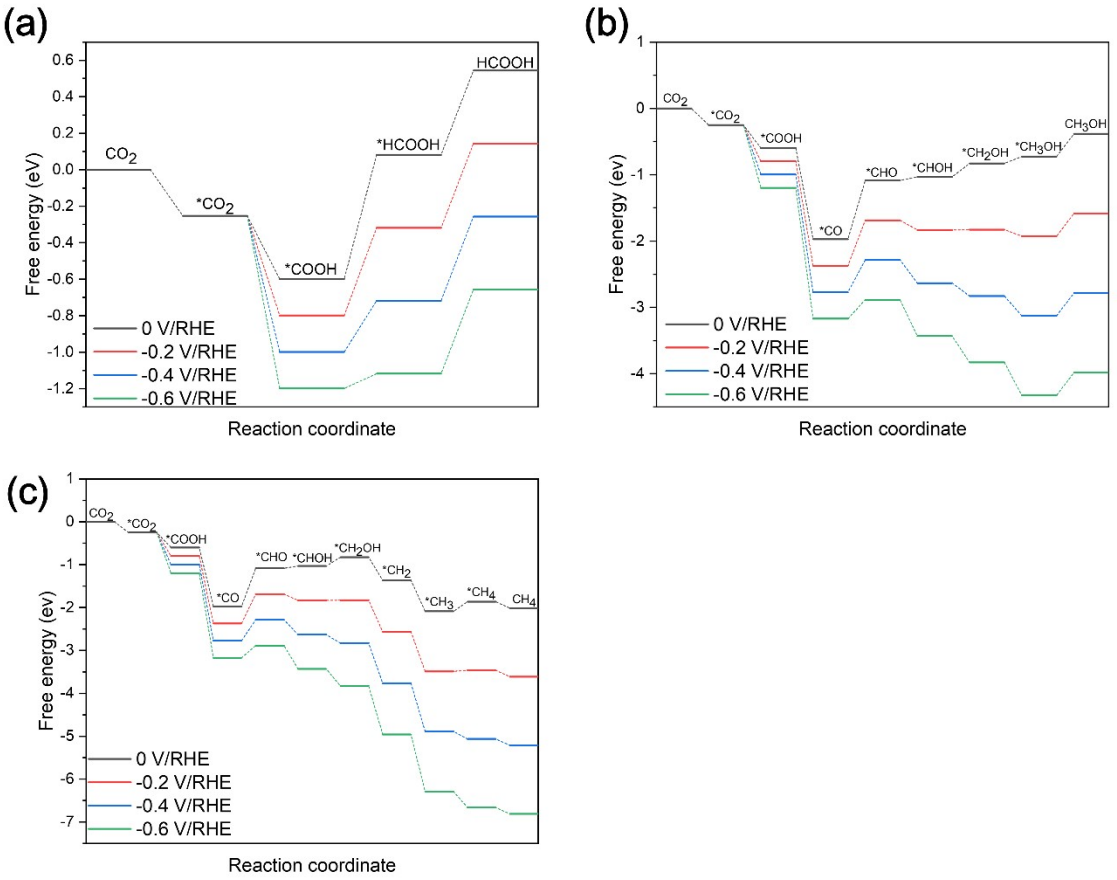

Fig.S5 The Gibbs free energy pathways graph to (a) HCOOH (b) CH_3OH (c) CH_4 via CO_2RR on Ru-pdGY under various applied external potentials.

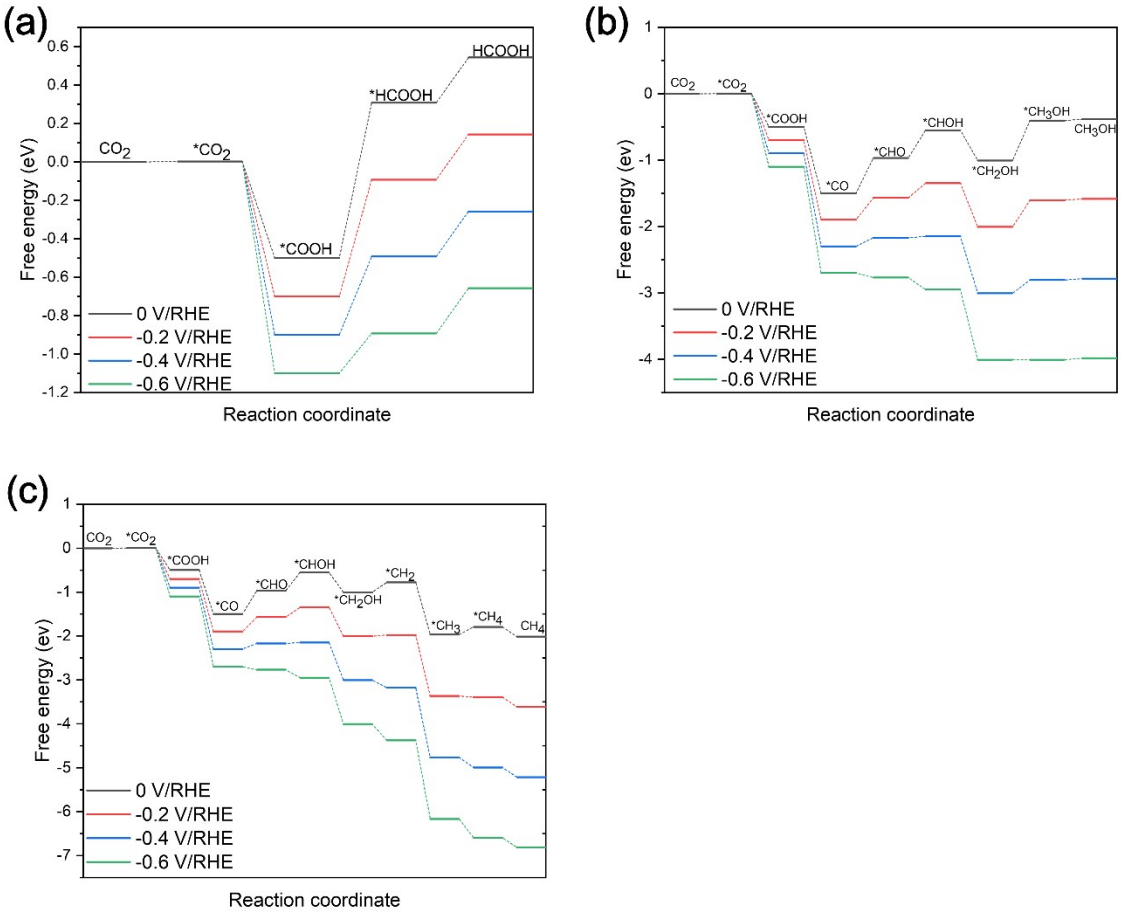

Fig.S6 The Gibbs free energy pathways graph to (a) HCOOH (b) CH_3OH (c) CH_4 via CO_2RR on Rh-pdGY under various applied external potentials.

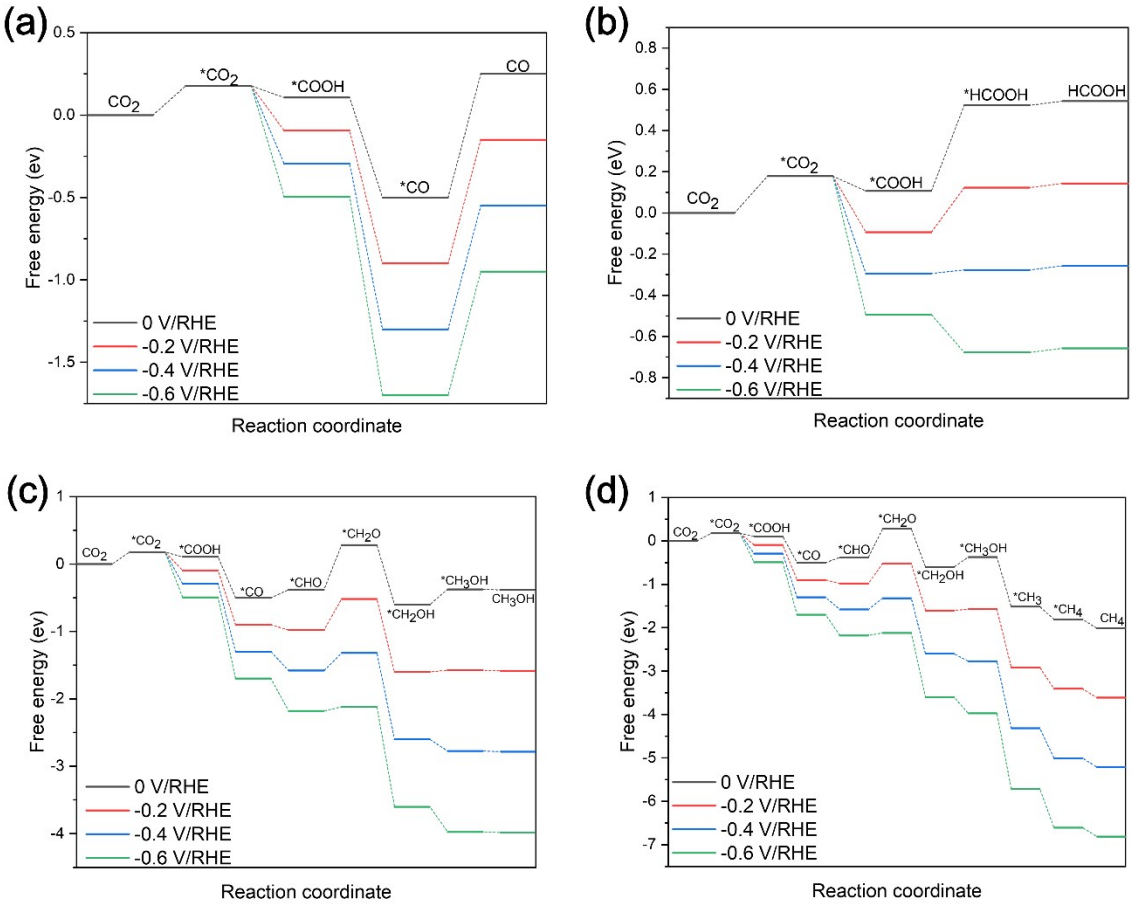

Fig.S7 The Gibbs free energy pathways graph to (a) CO (b) HCOOH (c) CH_3OH (d) CH_4 via CO_2RR on Pd-pdGY under various applied external potentials.

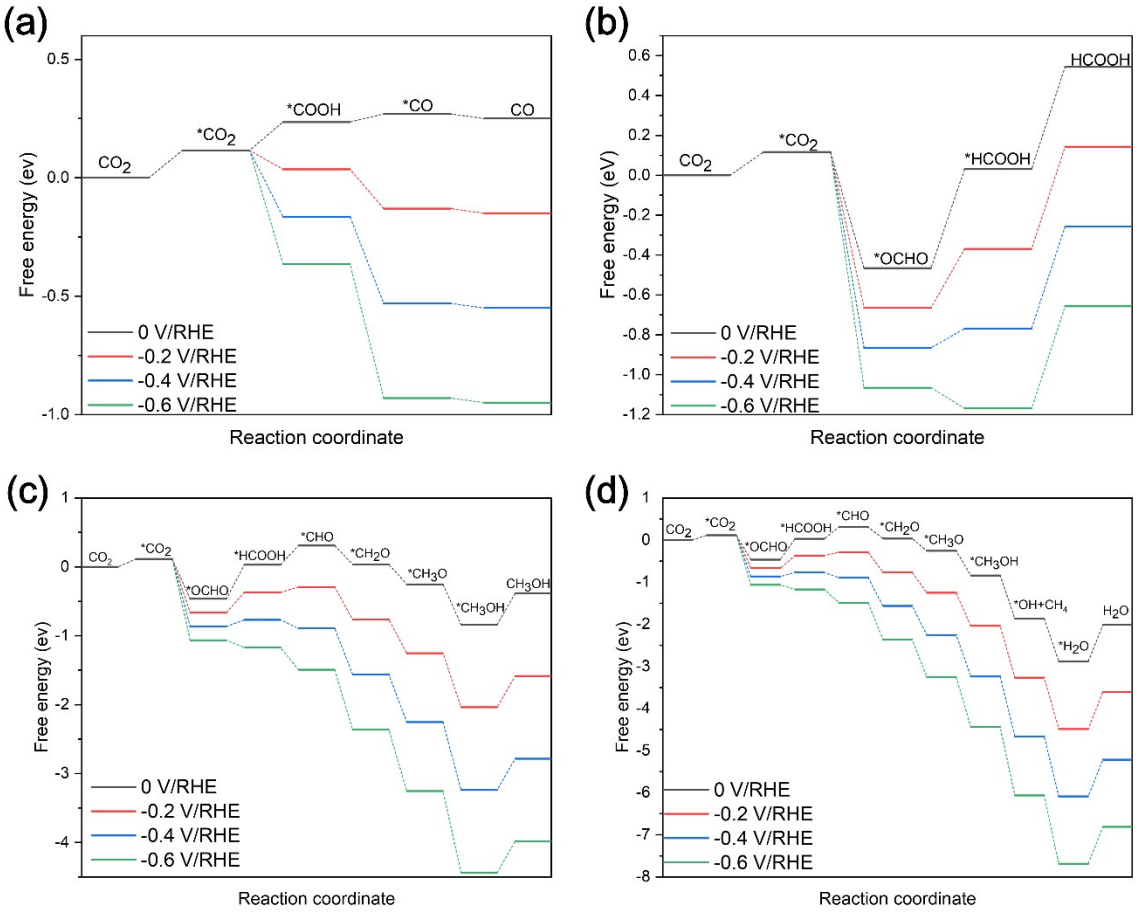

Fig.S8 The Gibbs free energy pathways graph to (a) CO (b) HCOOH (c) CH_3OH (d) CH_4 via CO_2RR on Cd-pdGY under various applied external potentials.